Title

Evaluation of Maxillary Skeletal and Dental Shape and Size in Patients with Palatally Impacted Maxillary Canines: A Cone Beam Computed Tomography Study

Author

Kasper, Stephen

Publication Date

2023

Peer reviewed|Thesis/dissertation

Evaluation of Maxillary Skeletal and Dental Shape and Size in Individuals with Palatally Impacted Maxillary Canines: A CBCT Study

by
Stephen Kasper

THESIS
Submitted in partial satisfaction of the requirements for degree of
MASTER OF SCIENCE

in

Oral and Craniofacial Sciences

in the

GRADUATE DIVISION
of the
UNIVERSITY OF CALIFORNIA, SAN FRANCISCO

Approved:

DocuSigned by:
Snehlata Oberoi ______________________ Snehlata Oberoi
5341FCF07489402...
Chair

DocuSigned by:
Nathan Young ______________________ Nathan Young
[illegible]404...

DocuSigned by:
David Hatcher ______________________ David Hatcher
B5404B44980A4A0...

____

____
Committee Members

Evaluation of Maxillary Skeletal and Dental Shape and Size in Patients with Palatally Impacted Maxillary Canines: A Cone Beam Computed Tomography Study

By Stephen Kasper

Abstract

Objective: This study investigated maxillary skeletal structures and dentition shape and size in subjects with palatally impacted maxillary canines using geometric morphometric analysis. Methods: In this cross sectional study, cone-beam computed tomography images for 40 subjects (22 females, 18 males, mean age 16 years) with palatally impacted canines and 40 subjects (22 females, 18 males, mean age 17 years) with nondisplaced canines were included from a single radiology center. On cone-beam computed tomography images the nasal cavity, palate, sinus, alveolar crest, maxillary lateral walls, and dentition were landmarked by three examiners. Landmarked CBCT images were evaluated for shape using geometric morphometric analysis by performing procrustes superimpositions and principle component analysis. Shape differences were further investigated by using logistic regression and linear regression analyses. Results: Principle component analysis revealed subjects with palatally impacted maxillary canines had a nasal cavity that was more constricted, the palate was more deeply vaulted and constricted, the sinus extended less vertically, canines were wider both mesial-distally and buccal-palatally in relation to length, and the lateral incisors were more narrow both mesial-distally and buccal-palatally in relation to length. Logistic regression depicted five variables that were associated with palatally impacted maxillary canines: Maxillary basal width at the first molar area, palatal depth, canine centroid size, lateral incisor centroid size, and central incisor centroid size ($p<.05$). Conclusions: In palatally displaced maxillary canines, both the canine and lateral

incisor size was diminished while the central incisor size was comparatively increased. The nasal cavity was constricted, the palate perimeter was constricted, the palate was more deeply vaulted, the sinus extended less vertically, and the basal maxillary width was constricted at the first molar area.

Table of Contents

List of Figures

List of Tables

Introduction

Background

The maxillary permanent canines are crucial in maintaining oral function, stability, and aesthetics (Yang). Calcification of the maxillary canines begins at 4-5 months, the crown is completely formed by 6-7 years of age, eruption occurs at 11-12 years of age, and root formation is complete by 12-15 years old (Ristaniemi). From its initial position, the canine migrates more than 22mm in a downward and forward direction to erupt adjacent to the distal aspect of the lateral incisor (Coulter). In the foundational study by Coulter, it was determined that the maxillary canine travels on average 11.8mm in the anterior-posterior direction, 18.56mm in the vertical direction, and 2.67mm in the lateral direction during its migration pathway. Many factors can prevent the proper eruption of the canine during its 22mm eruption pathway, and the canine can become impacted and remain embedded within soft or hard tissue (Dadgar). The maxillary permanent canines are the most frequently impacted teeth, with exception of the third molars. This condition has a prevalence of 1–2.5%. (Ericson and Kurol). They occur more frequently in females than in males (Aktan). Impacted maxillary canines are more frequently palatally positioned than buccally positioned, with palatal impactions accounting for 85% of all canine impactions (Ericson). Additionally, unilateral impacted maxillary canines are more common than bilateral impacted canines (Herrera et al.)

Several etiological factors have been suggested and explored for maxillary canine impaction. There are two prevailing theories for palatally impacted maxillary canines however, they are known as the “guidance theory” and the “genetic theory” (Becker). The guidance theory proposes that the maxillary canine lacks the proper guidance for eruption due to factors such as missing teeth, supernumerary teeth, or improper lateral incisor morphology (Listas). The genetic theory proposes that the maxillary canine becomes impacted due to the developmental disruption of the dental lamina (Peck).

Treatment

Early diagnosis of canine displacement and impaction is important because interceptive treatment of maxillary canine impaction can reduce treatment costs and time, decreases risks of complications and adverse outcomes, and facilitates orthodontic mechanics (Alqerban). Thus early detection is often the first approach in growing individuals so that the canine can be guided into its normal erupted position. It is suggested that patients be examined as early as the ages of eight or nine to assess the displacement of canines from their normal position. Radiographic and clinical evaluations (palpation and visual inspection) can be used to investigate the possibility of canine impaction (Shapira). If early canine impaction is suspected, treatment often consists of removal of the deciduous canines or is combined with creating spaces in the dental arch (Zuccati). Extraction of the primary canine is supported on the basis of the assumption that the primary canine would present as an obstacle in the eruption pathway of the permanent canine. In a study by Ericson and Kurol, they found that "if the crown of the permanent canine were distal to the midline of the later incisor root, the primary canine extraction normalized the erupting position of the permanent canine in 91% of the cases. In contrast, the success rate decreased to 64% if the permanent canine crown were mesial to the midline of the lateral incisor root" (Ericson).

Maxillary expansion is another treatment option in the early mixed dentition period. In a study conducted by Baccetti, "rapid maxillary expansion protocol was applied and according to their results the prevalence rate of successful eruption (65.7%) in the treatment group was significantly higher ($p<0.001$) than the control group (13.6%). Space for the maxillary permanent canine can also be created by distalizaion, with devices such as headgear, or by extraction of maxillary deciduous first molars (Nieri). If these different interceptive treatments fail, or if early detection of an impacted canine fails, surgical exposure of the impacted canine is essential, usually requiring a combination of surgical and orthodontic interventions to bring the canine successfully into the dental arch. Therefore, older patients with impacted canines require more time and are more difficult to treat than younger patients (Becker).

Current Diagnosis

To be able to properly provide interceptive treatment and avoid more arduous treatment such as surgery, the clinician must be able to proper predict and diagnose impaction early in a patient's development. In a literature review published by Listas et al., surveyed from 1996 to May of 2010, it was found that current models used to predict canine impaction are based on two dimensional radiographs (panoramic and AP Cephalometric radiographs) and clinical measurements. Clincally, several studies have investigated the relationship between a maxillary transverse discrepancy and palatally impacted maxillary canines, however the findings of these studies have been conflicting. In one study by Langberg and Peck, they compared the pre-treatment arch widths (measured clinically) of 10 males and 21 females in the permanent dentition with palatally displaced canines to the arch widths of an unaffected group of orthodontic patients with the same age and sex distribution. They did not find any statistical differences between the two groups both in the anterior and the posterior maxillary width (Langberg). Conversely, in a study by

Mc Connell *et al.,* they found that a transverse maxillary deficiency in the anterior portion of the dental arch as a local cause for palatal canine displacement. In their study "Inter-molar and inter-canine widths were recorded in 57 patients with 81 impacted maxillary canines and in 103 patients with normally erupted canines that served as a control group. Their results demonstrated statistically significant differences ($p<0.05$) in the maxillary width between the two groups, particularly in the anterior portion of the maxilla" (Mc Connell).

Radiographically, two dimensional radiographs including panoramic imaging and AP cephalograms have been used to assess and predict displaced canines in the mixed dentition period. "Three variables visible on panoramic radiographs have been proposed (to predict canine impaction): I) angle measured between the long axis of the impacted canine and the midline. II) distance between the canine cusp tip and the occlusal plane (from the first molar to the incisal edge of the central incisor) and III) the sector where the cusp of the impacted canine is located" (Ericson). In one retrospective study of 554 maxillary canines of children between 4 and 12 years old, investigators discovered that when the lateral incisor is not yet fully developed, panoramic radiographs show 67% overlapping of the canine and lateral incisor. However, when lateral incisor development is complete, only 11% of the subjects show some degree of overlapping. "According to the authors, the overlapping of the canine and lateral incisor can be considered as a sign of early canine displacement after the incisor has completed its root development" (Fernandez). On PA radiographs, one study suggested that, "At the age of 8, the maxillary canines should have medial inclination with crowns below the lateral border of the nasal cavity and the roots lateral to the border of the nasal cavity. Some parameters such as intercanine width, size of the follicle, symmetry and width of the nasal cavity might be associated with increased probability of upper canine impaction" (Sambataro). These two dimensional radiographic methods and the aforementioned clinical measurements have served as the gold standard for years for assessing and predicting maxillary canine impaction.

Cone-Beam Computed Tomography

While the use of two dimensional radiographs for diagnosis has proven useful, panoramic radiographs are inherently technique sensitive and prone to distortion. In particular, panoramic image mesiodistal angles have been proven to be significantly different from true angle measurements (Mckee). In one study by Haney, they compared traditional two dimensional images to CBCT images in patients with maxillary impacted canines. They found that there was a 21% disagreement in the mesio-distal location and a 16% disagreement in the labial-palatal position of the impaction. Therefore while useful, previous models using two-dimensional radiographs are inherently flawed. CBCT imaging provides a much more precise tool to locate impacted canines and factors associated with impacted canines. Current maxillary canine impaction models, which use panoramic imaging, could greatly benefit from CBCT imaging. Creating a prediction model using CBCT imaging would increase accuracy in early diagnosis and interceptive treatment of maxillary canine impaction.

While CBCT imaging has been around for over two decades, only until recently has the use of this imaging modality become more affordable and common amongst the common orthodontic practice. With the widespread use of CBCT imaging and its added benefits, it is becoming increasingly important to conduct more studies using three dimensions. In the last few years studies using CBCT imaging to evaluate the etiology of maxillary canine impaction have emerged. While these studies have evaluated factors associated with maxillary canine impaction, such as later incisor root resorption and position of adjacent teeth, no three dimensional study exists that provides a comprehensive evaluation of factors associated with maxillary canine impaction. Therefore this study will aim to evaluate both skeletal and dental factors associated with palatally impacted maxillary canines using CBCT imaging.

Geometric Morphometric Analysis

The three-dimensionality of CBCT imaging provides the unique opportunity to not only evaluate where objects are in relation to one another in a 3D sphere, but also allows for the evaluation of shape and size. In the literature, geometric morphometrics (GMM) has been proposed as a effective method of visualization of shape changes (Papagiannis). "This method can show three-dimensional (3D) morphological changes in their complexity much more effectively than coefficients resulted from traditional morphometric analysis" (Klienberg). The geometric morphometrics method (GMM) is a technique to study scale and shape relationships of structures using Cartesian geometric coordinates rather than linear, areal (of area), or volumetric variables (Liuti). Therefore to gain a deeper understanding of maxillary canine impaction, geometric morphometric analysis can be used with CBCT imaging.

Central Hypothesis

We hypothesize that there is an association between the size and shape of the maxillary dentition, palate, nasal cavity, sinus, and maxillary arch in the palatal impaction of maxillary canines.

Specific Aims

1. Evaluate maxillary canine and adjacent teeth size, shape, and orientation.
2. Evaluate maxillary alveolar bone thickness and maxillary basal width.
3. Evaluate maxillary nasal cavity width and shape.
4. Evaluate palatal vault dimensions and shape.
5. Evaluate maxillary sinus shape and dimensions.
6. Explore arch widths and lengths
7. Compare the above studied variables between palatally displaced maxillary canines and nondisplaced canines.
8. Determine the effect of studied variables on the position of canine displacement.

Materials and Methods

This cross sectional study evaluates the factors associated with palatally impacted maxillary canines compared to subjects that have non-displaced maxillary canines using CBCT images. This study was conducted at the University of California, San Francisco in conjunction with a radiology center in Sacramento, California. All CBCT images were obtained from the same radiology center and same CBCT machine, with all images taken between March 2021 and November 2022. The CBCT images were screened for the presence of palatally impacted maxillary canines, with inclusion criteria including aged greater than 12 years (The maxillary canine is on average fully erupted by ages 11-12) and a clinically diagnosed unilateral or bilateral maxillary canine impaction. Exclusion criteria were poor image quality, syndromic and cleft patients, prior orthodontic treatment or early extractions, root canal treatment, and presence of cysts or other pathologies.

This cross sectional study consisted of 80 total subjects (44 females and 36 males), 40 "impaction" subjects (22 females, 18 males, mean age 16 years) with palatally impacted canines and 40 "control" subjects (22 females, 18 males, mean age 17 years) with nondisplaced canines. All subjects were between the ages of 12 and 19 years old. All CBCT data (DICOM files) were assigned new names by using randomly generated codes that removed patient identification information. After de-identification, all subject DICOM files were uploaded into Stratovan Checkpoint's land-marking software.

A template of 146 landmarks was created to adequately represent the maxillary dentition, palate, nasal cavity, sinus, and maxillary arch. In selecting landmarks to plot, this study aimed to identify landmarks that would depict adjacent structures and the housing within which the maxillary permanent canine travels during its eruption pathway. Table I represents the various landmarks and their definitions.

Table I. Landmark Definitions

Table I. Landmark Definitions	
Quantitative Variables	*Values and definition*
Dental Measurements	
MD (tooth mesiodistal width)	Maximum mesiodistal crown diameter of maxillary anterior teeth (U1, U2, U3,U4,U5,U6)
BL (tooth buccolingual width)	Maximum buccolingual crown diameter of maxillary anterior teeth (U1, U2, U3,U4,U5,U6)
TA (Tip-Apex)	Maxium tooth legnth measured from root apex to crown cusp tip (U1,U2,U3,U4,U5,U6)
Alveolar Ridge Landmarks	
#Crest_(B/P)	Buccal Lingual width of U1,2,4,5,6 measured from height of alveolar ridge buccal and lingual
Arch Widths	
IP1 (anterior dental arch width)	Intermaxillary arch width between the deepest points of the Distal fossae of the maxillary first premolars (IP1)
IM1 (posterior dental arch width)	Intermaxillary arch width between mesial lingual cusp tips first molars (IM1)
Nasal Cavity Landmarks	
Anterior Limit (ANC)	Defined by the most anterior portion of the piriform aperture with a continuous cortex
ANC_Inf	Most inferior middle point
ANC_Lat_(R/L)	Most lateral limits of nasal cavity on both left and right
Posterior Limit (PNC)	Defined by the posterior nasal spine
PNS	Most inferior posterior point of palate
PNC_Lat_(R/L)	Most lateral limits of nasal cavity on both left and right
Maxillary Transverse Width	
M1_Basal_(R/L)	First molar basal width (at level of floor of nasal cavity)
M1_Alveolar_(R/L)	First molar alveolar width (at level of heigh of alveolar ridge)
P1_Basal_(R/L)	First premolar basal width (at level of palate)
P1_Alveolar_(R/L)	First premolar alveolar width (at level of heigh of alveolar ridge)
Patatal Landmarks	
Palate Boundaries	a. 9 points on Mid-sagital suture (Defined as "MS_#") c. Distal boarder: 9 points distal to first molars perpendicular to Mid-sagittal suture (Defined as "Distal Border Palate (DBP_#)")
Maxillary sinus Landmarks	
Sinus Floor # (R/L)	9 points on the floor of the maxillary sinus from the distal of the first molar to most anterior portion of sinus in A-P (Sinus_#)

For each of the landmarks, a standardized protocol and orientation was established in order to be able to reliabily replicate and place landmarks. A total of three examiners landmarked the CBCT data in Stratovan Checkpoint using the aforementioned template consisting of 146 landmarks. Prior to landmarking the 80 cases, each examiner landmarked 5 of the same cases to evaluate inter-rater reliability and agreement using within subject standard deviations and agreement analysis. There were a total of 9 errors where one examiner diagreed with the others by greater than 0.5mm and therefore required correction (out of 6570) measurements. It was determined that there was a high level of agreement amognst the examiners. Tables II and III depict the various numerical landmarks and the error (in mm) between the three examiners.

Table II. Numerical Values

Table II. Numerical Landmarks

1	UR1_M	21	UR3_A	41	UR6_B	61	UL2Crest_B	81	UL5_A	101	PNC_Lat_R	121	DBP_2	141	Sinus_L4
2	UR1_D	22	UR3_T	42	UR6_P	62	UL2Crest_P	82	UL5_T	102	PNC_Lat_L	122	DBP_3	142	Sinus_L5
3	UR1_P	23	UR4_M	43	UR6_A	63	UL3_M	83	UL5Crest_B	103	M1_Basal_R	123	DBP_4	143	Sinus_L6
4	UR1_B	24	UR4_D	44	UR6_T	64	UL3_D	84	UL5Crest_P	104	M1_Basal_L	124	DBP_5	144	Sinus_L7
5	UR1_A	25	UR4_P	45	UR6Crest_B	65	UL3_B	85	UL6_M	105	M1_Alveolar_R	125	DBP_6	145	Sinus_L8
6	UR1_T	26	UR4_B	46	UR6Crest_P	66	UL3_P	86	UL6_D	106	M1_Alveolar_L	126	DBP_7	146	Sinus_L9
7	UR1Crest_B	27	UR4_A	47	UL1_M	67	UL3_A	87	UL6_B	107	P1_Basal_R	127	DBP_8		
8	UR1Crest_P	28	UR4_T	48	UL1_D	68	UL3_T	88	UL6_P	108	P1_Basal_L	128	DBP_9		
9	UR2_M	29	UR4Crest_B	49	UL1_B	69	UL4_M	89	UL6_A	109	P1_Alveolar_R	129	Sinus_R1		
10	UR2_D	30	UR4Crest_P	50	UL1_P	70	UL4_D	90	UL6_T	110	P1_Alveolar_L	130	Sinus_R2		
11	UR2_B	31	UR5_M	51	UL1_A	71	UL4_B	91	UL6Crest_B	111	MS_1	131	Sinus_R3		
12	UR2_P	32	UR5_D	52	UL1_T	72	UL4_P	92	UL6Crest_P	112	MS_2	132	Sinus_R4		
13	UR2_A	33	UR5_P	53	UL1Crest_P	73	UL4_A	93	IP1_R	113	MS_3	133	Sinus_R5		
14	UR2_T	34	UR5_B	54	UL1Crest_B	74	UL4_T	94	IP1_L	114	MS_4	134	Sinus_R6		
15	UR2Crest_P	35	UR5_A	55	UL2_M	75	UL4Crest_B	95	IM1_R	115	MS_5	135	Sinus_R7		
16	UR2Crest_B	36	UR5_T	56	UL2_D	76	UL4Crest_P	96	IM1_L	116	MS_6	136	Sinus_R8		
17	UR3_M	37	UR5Crest_B	57	UL2_B	77	UL5_M	97	ANC_Inf	117	MS_7	137	Sinus_R9		
18	UR3_D	38	UR5Crest_P	58	UL2_P	78	UL5_D	98	ANC_Lat_R	118	MS_8	138	Sinus_L1		
19	UR3_P	39	UR6_M	59	UL2_A	79	UL5_B	99	ANC_Lat_L	119	MS_9	139	Sinus_L2		
20	UR3_B	40	UR6_D	60	UL2_T	80	UL5_P	100	PNS	120	DBP_1	140	Sinus_L3		

Table III. Inter-rater Analyis (error in mm)

Table III. Inter-rater analysis

Landmark	Error	Landmark	Error	Landmark	Error	Landmark	Error	Landmark
MS_5	0.36788848	UL2_P	0.18777025	DBP_2	0.13035362	UR4Crest_P	0.09911811	UL6_A
UL3_M	0.35722038	UL2_M	0.18765927	UL4_M	0.12979985	UR5_D	0.09870934	UL5_M
UR3_P	0.33199367	Sinus_R8	0.18612397	Sinus_L7	0.12765474	UR4Crest_B	0.09811898	UR6_P
MS_7	0.31991905	Sinus_L3	0.18138118	UR3_A	0.12526026	M1_Alveolar_R	0.09770295	UL6_P
UR3_B	0.31224125	UL2_D	0.17987106	UR4_D	0.12338152	MS_8	0.09769476	UL5_P
UR3_D	0.30842384	UL2_B	0.17652441	UL6_D	0.12211879	UL4_D	0.09766234	Sinus_R2
ANC_Lat_L	0.30272826	PNC_Lat_R	0.1733309	IP1_L	0.11724106	Sinus_L9	0.09742043	UL2_T
UL3_D	0.29517362	Sinus_L4	0.17072161	DBP_4	0.11666819	UL1_M	0.09734132	UR2Crest_P
MS_4	0.29508903	UL2_A	0.16994019	UL4_B	0.11403859	DBP_8	0.09707386	UR4_M
MS_3	0.2897087	Sinus_R7	0.16589475	UR2Crest_B	0.11337783	PNS	0.09704707	UR1_A
UL1Crest_B	0.27906893	UL6_T	0.16589173	UR5_A	0.11241323	Sinus_R1	0.09637427	UL1_T
UR3_M	0.27240117	IM1_L	0.16457967	UR6_B	0.11057155	UR5_M	0.0954966	UL5_T
M1_Basal_L	0.2682843	Sinus_L2	0.16336034	UL4_A	0.10834359	UR1_D	0.09508943	UL1_P
UR1Crest_P	0.26388571	MS_9	0.16300307	UR6Crest_B	0.10830789	UL6Crest_P	0.09480331	UR5_B
MS_6	0.26272673	UL4Crest_B	0.16113266	P1_Alveolar_R	0.10641554	UL6_B	0.09370984	UL1_B
ANC_Lat_R	0.26229652	Sinus_R6	0.16015763	DBP_3	0.10538849	UL5_D	0.09174239	IP1_R
UR1Crest_B	0.2572949	UR2_M	0.15667738	DBP_1	0.10537615	DBP_5	0.09103845	UR5_T
UL1Crest_P	0.25143442	IM1_R	0.15172914	UL4Crest_P	0.10335247	UR4_P	0.08941775	UR4_B
UL3_P	0.22260638	UL1_D	0.1478754	UR6Crest_P	0.10315038	UL5Crest_P	0.08909807	UL4_T
UL3_B	0.21182823	Sinus_L5	0.14756219	UR6_M	0.10306341	UR1_M	0.0875694	UR5_P
P1_Basal_L	0.20562685	DBP_7	0.14623725	DBP_9	0.1029686	UR2_P	0.08748143	UR5Crest_B
UR1_B	0.20294367	UL6Crest_B	0.14292865	Sinus_R3	0.10285815	UR6_T	0.08716957	UR2_T
UR1_P	0.20200363	Sinus_R9	0.14274826	UR6_A	0.10275213	UR2_B	0.0869977	UL3_T
UR6_D	0.20185027	Sinus_R4	0.14143173	MS_2	0.10240866	UR2_A	0.08362376	UR3_T
UL3_A	0.20180172	Sinus_L1	0.14087701	P1_Basal_R	0.10066148	UR4_A	0.08338385	UR1_T
M1_Basal_R	0.20026266	P1_Alveolar_L	0.13815764	Sinus_L8	0.10053623	UL4_P	0.0830538	UR4_T
UL2Crest_P	0.19412092	ANC_Inf	0.13736957	UR2_D	0.10006798	MS_1	0.08302329	
PNC_Lat_L	0.19224099	Sinus_L6	0.13735768	UL1_A	0.09933345	UL5_B	0.0826422	
UL2Crest_B	0.19005701	M1_Alveolar_L	0.13506073	UL5Crest_B	0.09918736	DBP_6	0.08213607	
UL5_A	0.18924887	Sinus_R5	0.13044846	UL6_M	0.09918266	UR5Crest_P	0.07999292	

The following figures 1-6 depict the orientations used to plot dental landmarks, nasal cavity landmarks, palate landmarks, alveolar landmarks, and sinus landmarks.

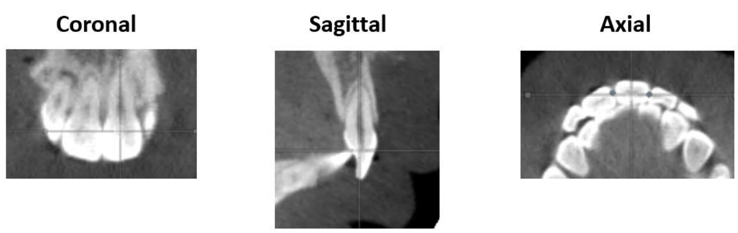

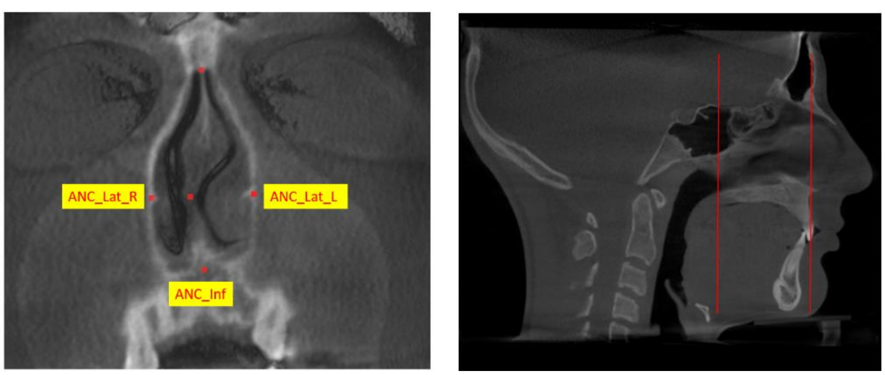

Figure 1. Dental Orientation (Above), Figure 2. Nasal Cavity Orientation (Below)

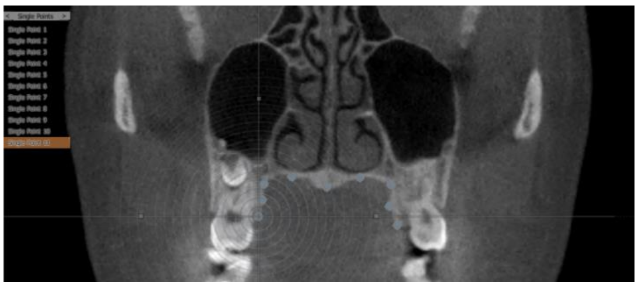

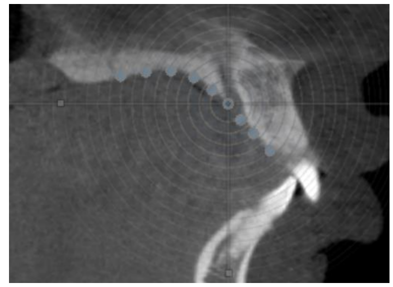

Figure 3. Patale Orientation (Above), Figure 4. Alveolar Orientation (Bottom Left),

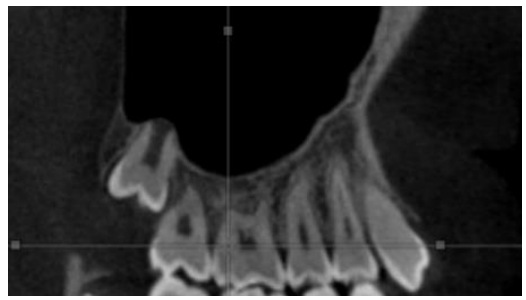

Figure 5. Sinus Orientation (Bottom Right).

After all 80 cases were landmarked in Stratovan Checkpoint, landmarked 3D data points were then transferred to MorphoJ Geometric Morphometric software (Klingenberg lab, Manchester, UK) to standardize the superimpositions across all subjects in this study, generating a list of procrustes coordinates that control for scalar differences between images. Principal component analysis (PCA) was then completed using MorphoJ software. Following the PCA shape analysis a logistic regression and linear regressions were run against significant factors as determined and selected from the pricinpal component analysis results.

Results

Landmarks were converted into procrustes coordinates using MorphoJ software to control for scalar, translational, and rotational differences. Procrustes coordinates were graphed in MorphoJ and represented in 2D across 3 axes (see figure 6). A principal component analysis was then performed on the newly adjusted procrustes coordinates while selecting for impaction v control groups.

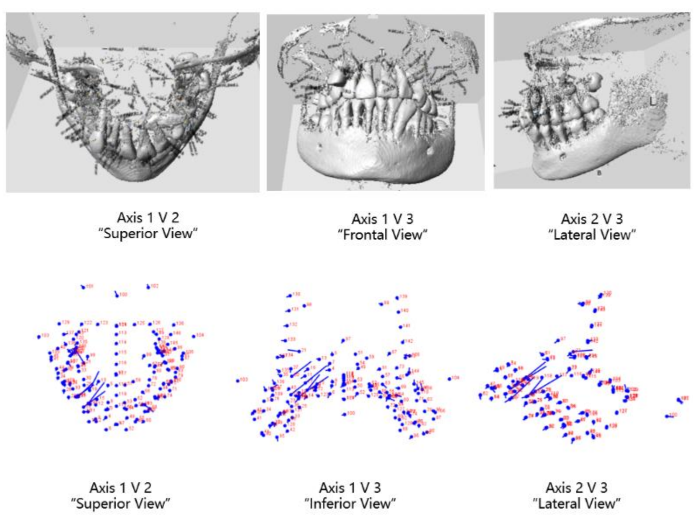

Figure 6. Proctrustes Coordinates

The first principle component graphed against the second principle component revealed a tight clustering of the impaction v control group, with 27% of the shape variation being attribiuted to the first two prinicple compents as obtained from the eigenvalues. This is depicted in Figure 7.

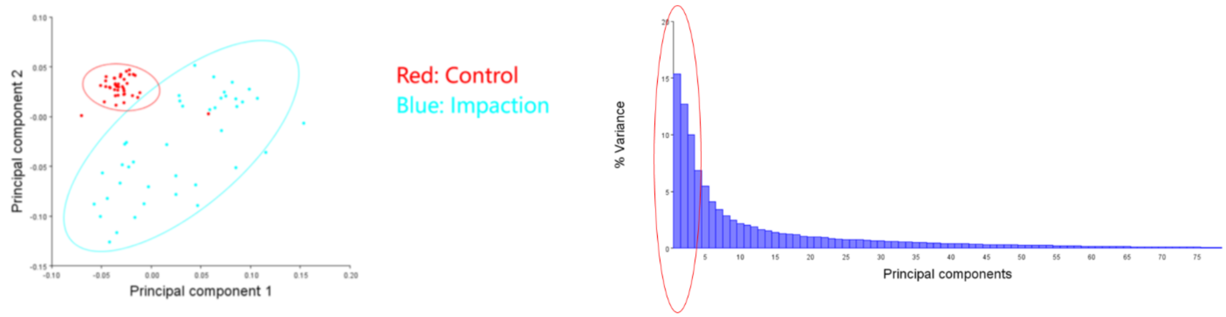

Figure 7. Principal Compenent Analysis all Landmarks

Due to the large number of landmarks, a principle compoenent analaysis was then performed for only the skeletal landmarks (landmark numbers 97-146) to further differentiate associative factors in palatally impacted maxillary canines. The skeletal landmarks involved in the PCA analyis include nasal cavity, palate, sinus, and maxillary arch landmarks. The first and second principal component analysis acounted for 35% of the total shape variation, with PC1 comprising 19% and PC2 comprising 16% of the total variation. To beter visualize the shape differences in these PCA grpahs, a wireframe network was created to connect the separate skeletal compnents. The starting shape is shown as a light blue outline with hollow dots at the positions of the landmarks, and the target shape is represented by darkblue outlines in these wireframe graphs. The wireframe graph of PCA 2 with a scale factor of -0.1 is included in Figure 8.

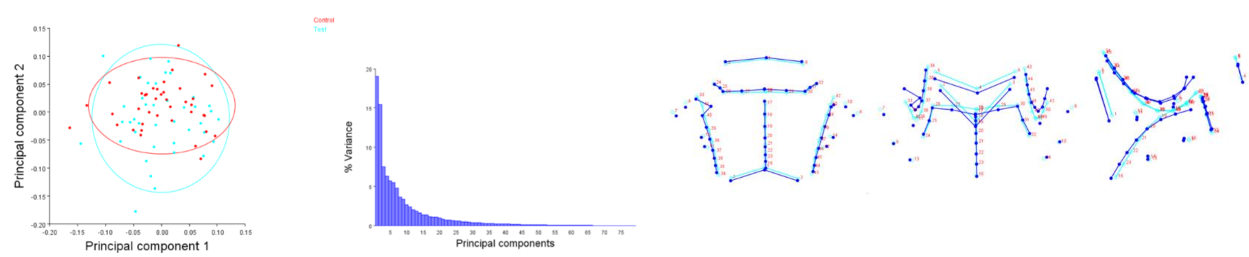

Figure 8. Skeletal landmarks PCA graph, and PCA 2 wireframe graph

Due to the large volume of skeletal landmarks, we decided to run indvidual principal component analyses on each separate skeletal and dental landmark, grouping for impaction v control subjects. The separate principal compenet analyses included the anterior nasal cavity, posterior nasal cavity, midsagittal suture of palate, posterior border of the patale, perimeter of the palate, sinus floor, the canine, the lateral incisor, the central incisor, the first premolar, the second premolar, and the first molar. As the PCA 2 wireframe graph of all the skeletal landmarks revealed noticeable shape differences, we decided to also create wireframe graphs for each individual principal component analysis to better visualize the shape changes occuring. Figures 9-21 depict the PCA and wire frame analyses using the first principal component and appropriate scaling factors were then generated for these separate components.

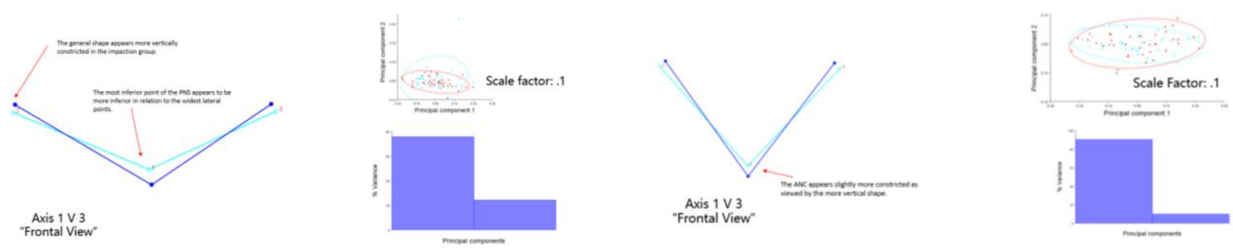

Figure 9. (Left) Posterior Nasal Cavity PCA, (Right) Anterior Nasal Cavity PCA

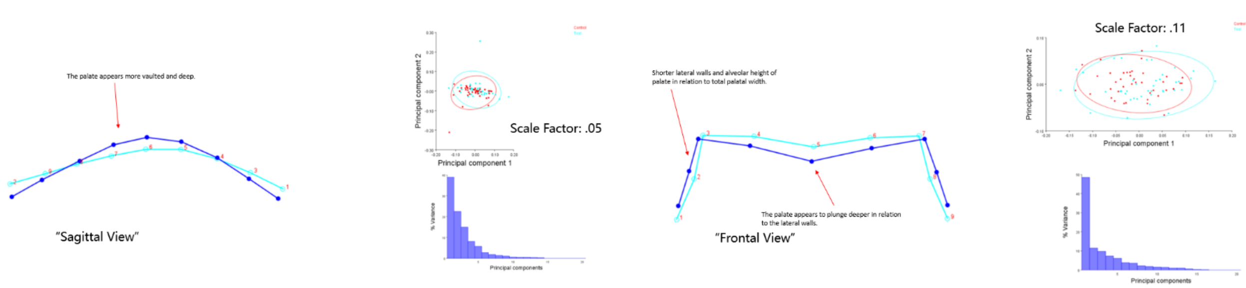

Figure 10. (Left) Midsagittal Suture of Palate PCA, (Right) Distal Border of Palate PCA

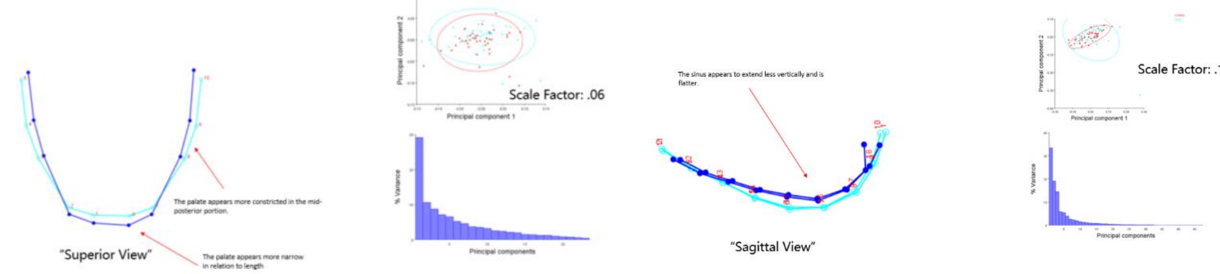

Figure 11. (Left) Perimeter of the Palate PCA, (Right) Sinus Floor PCA

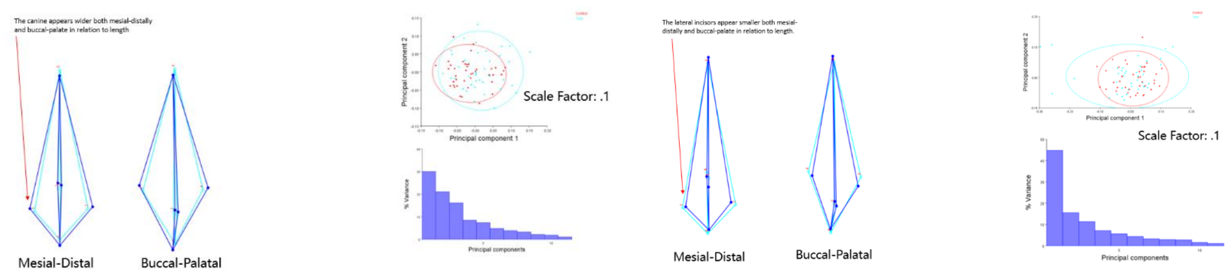

Figure 12. (Left) Canine PCA, (Right) Lateral Incisor PCA

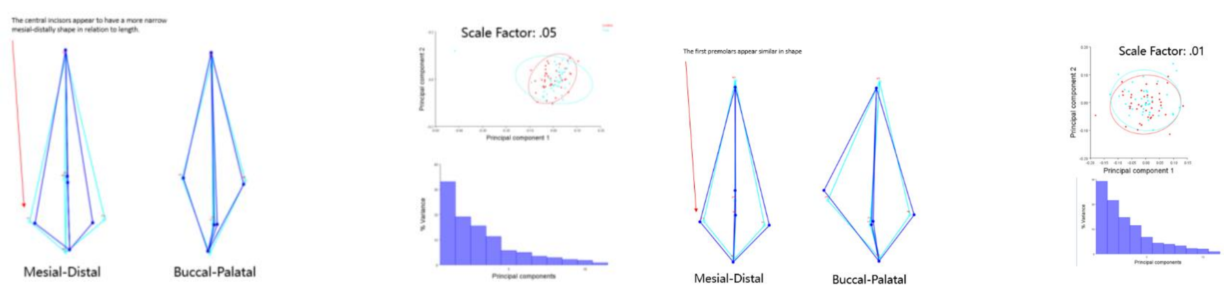

Figure 13. (Left) Central Incisor PCA, (Right) First Premolar PCA

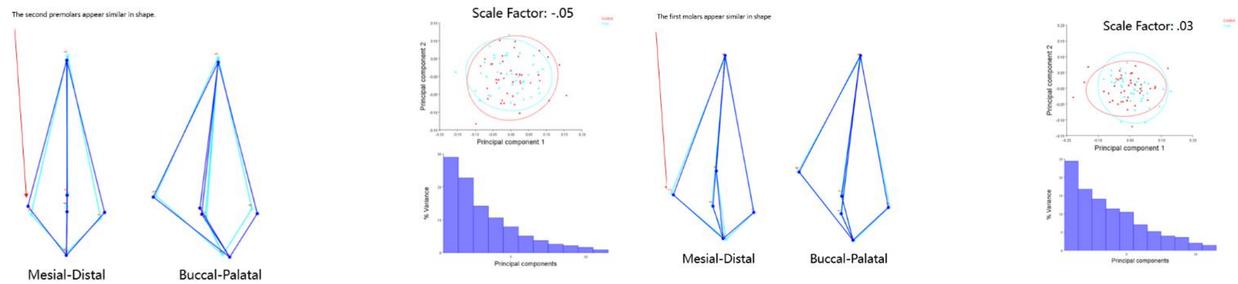

Figure 14. (Left) Second Premolar PCA, (Right) First Molar PCA

The various principal component analyses depict shape the shape changes from impaction and control groups. From these separate PCA graphs, 12 variables were identified as potentially significant variables associated with patalatally impacted maxillary canines. A logistic regression was then performed on these 12 variables, to determine the probabilty of an event of impaction occuring. Additionally an odds ratio was calculated for all of the 12 variables to determine the stregnth of the association. After controling for collineratity, the logistic regression revealed 5 significant factors associated with canine impaction with a total AIC value of 86.28. The first variable of significance was the total maxillary basal width at the area of the first molar, specifically at the height of the alveolar crest in this region. The estimated std. was -3.485 with a p value of 0.028 and an odds ratio of 0.706. The scond variable of significance was palatal depth with an estimated std. of 4.774, with a p value of 0.028 and an odds ratio of 1.610. The thrid variable of significance was canine centroid size with an estimated std. of -5.107, with a p value of 0.023 and an odds ratio of 0.601. The fourth variable of significance was laterial incisor centroid size with an estimated std. of -8.016, with a p value of 0.014 and an odds ratio of 0.450. The fifth variable of significance was central incisor centroid size with an estimated std. of 9.708, with a p value of 0.007 and an odds ratio of 2.632. The results are displayed in Table IV.

Table IV. Logistic Regression

Table IV				
Id	Estimated Std.	Std. Error	P Value	Odds Ratio
AM1_w	-3.485	1.596	0.028	0.706
Palate_h	4.775	2.184	0.028	1.610
Canine_c	-5.107	2.578	0.023	0.601
Lateral_c	-8.016	3.286	0.014	0.450
Central_c	9.708	3.657	0.007	2.632

Discussion

While previous studies have used two dimensional radiographs, and have primarily focused on canine angulations and sectors, this study provides valuable information about shape and size associations with palatally impacted maxillary canines. Prior to this study there was limited information on the association of skeletal and dental shape and size with the palatal impaction of maxillary canines. The use of CBCT imaging and geometric morphometric analysis provides valuable insight to the overall skeletal housing and contributing factors associated with palatally impacted maxillary canines.

The age of included subjects in this study was at least 12 years to allow the normal time needed for the maxillary canine to fully erupt into its final position. The 146 landmarks encompassed the maxillary dentation and the skeletal housing through which the canine migrates during its eruption pathway. Principle component analysis of the entire data set revealed a tight clustering of the control v impaction groups, indicative of significant shape differences between the two groups. The majority of the shape variation within this PCA was found within the first three principal components. While the analysis was useful in establishing shape differences between the two groups, the large volume of landmarks made visualization of the exact shape differences difficult. Therefore to further specify our shape analysis, another principal component analysis was performed on only the skeletal landmarks (landmarks 97-146). The majority of shape variance was found in the first two principal components. The most shape variance was found within the second PCA, with visible shape changes in the nasal cavity, sinus, maxillary arch, and palate.

To further specify the shape analysis from the skeletal PCA results, separate principal component analyses were conducted individually for the anterior nasal cavity, posterior nasal cavity, midsagittal suture of palate, posterior border of the patale, perimeter of the palate, sinus floor, the canine, the lateral incisor, the central incisor, the first premolar, the second premolar, and the first molar. The findings from the individual principal component anlaysis revealed the following shape differences in the impaction group v the control group. The posterior nasal cavity appears more vertically constricted in the impaction group. The anterior nasal cavity appears slightly more vertically constricted in the impaction group. The palate along the mid sagittal suture appears to be more vaulted in the impaction group. The palatal perimeter appears more narrow in relation to length in the impaction group. The sinus appears to extend less vertically and is flatter in shape in the impaction group. The canine appears wider both mesial-distally and buccal-palatally in relation to length in the impaction group. The lateral incisors appear smaller both mesial-distally and buccal-palatally in relation to length in the impaction group. The central incisors appear to have a more narrow mesial-distal shape in relation to length in the impaction group. The first premolars, second premolars, and first molars appear similar in shape in both the impaction and control group. The visualization of these differences in shape can be seen in figures 9-14.

The findings from the various principal component analyses delineated various factors of significance found in individuals with palatally impacted maxillary canines. Factors with the most variation from the PCA were compiled in a table and a logistic regression and odds ratio were generated to estimate the event of impaction occurring as well as the strength of the association between events. The logistical regression found that there is a negative association between increased total alveolar width at the first molar and canine impaction. There is a positive association between increased palatal depth and canine impaction. There is a negative association between increased canine centroid size and canine impaction. There is a negative association between increased lateral incisor centroid size and canine impaction. There is a positive association between increased central incisor centroid size and canine impaction.

In conclusion, this study supports the guidance theory in that a smaller than normal lateral incisor lacks sufficient surface area to guide the maxillary canine into its proper occlusion. Diminished canine size and a relatively broader mesial-distal dimension (in relation to length) is associated with a higher prevalence of impaction. A deep palatal vault and narrow nasal cavity is associated with impaction. This may lead to an increase of space palatally, and as the canine erupts, the pathway of least resistance would lead to palatal impaction. A constricted total maxillary alveolar width, specifically at the first molar is associated with impaction. This constriction may direct the canine inward, leading to palatal impaction. And lastly, a shallow sinus is associated with impaction and may pose a vertical problem which thereby influences the canine eruption pathway.

Bibliography

1. Yang S, Yang X, Jin A, et al. Sequential traction of a labio-palatal horizontally impacted maxillary canine with a custom three directional force device in the space of a missing ipsilateral first premolar. Korean J Orthod 2019;49(02):124–136
2. Ristaniemi J, Rajala W, Karjalainen T, Melaluoto E, Iivari J, Pesonen P, Lähdesmäki R. Eruption pattern of the maxillary canines: features of natural eruption seen in PTG at the late mixed stage-Part I. Eur Arch Paediatr Dent. 2022 Apr;23(2):223-232. doi: 10.1007/s40368-021-00650-1. Epub 2021 Jul 14. PMID: 34263432; PMCID: PMC8994718.
3. Coulter J, Richardson A. Normal eruption of the maxillary canine quantified in three dimensions. Eur J Orthod 1997;19:171-83.
4. Dadgar S, Alimohamadi M, Rajabi N, Rakhshan V, Sobouti F. Associations among palatal impaction of canine, sella turcica bridging, and ponticulus posticus (atlas arcuate foramen). SurgRadiol Anat 2021;43(01):93–99
5. Becker A, Peck S, Peck L, Kataja M. Palatal canine displacement: guidance theory or an anomaly of genetic origin? Angle Orthod 1995;65:95–102
6. Bishara SE. Impacted maxillary canines: a review. Am J Orthod Dentofacial Orthop 1992;101:159-71
7. Peck S, Peck L, Kataja M. Concomitant occurrence of canine malposition and tooth agenesis: evidence of orofacial genetic fields. Am J Orthod Dentofacial Orthop 2002;122(06):657–660
8. Haney E, Gansky SA, Lee JS, et al. Comparative analysis of traditional radiographs and cone-beam computed tomography volumetric images in the diagnosis and treatment

planning of maxillary impacted canines. *Am J Orthod Dentofacial Orthop.* 2010;137:590–97.

9. Litsas G, Acar A. A review of early displaced maxillary canines: etiology, diagnosis and interceptive treatment. Open Dent J 2011; 5:39–47
10. John H Warford, Ram K Grandhi, Daniel E Tira, Prediction of maxillary canine impaction using sectors and angular measurement, American Journal of Orthodontics and Dentofacial Orthopedics, Volume 124, Issue 6, 2003, Pages 651-655, ISSN 0889-5406, https://doi.org/10.1016/S0889-5406(03)00621-8.
11. Mckee IW, Williamson PC, Lam EW, Heo G, Glover KE, Major PW. The accuracy of 4 panoramic units in the projection of mesiodistal tooth angulations. Am J Orthod Dentofacial Orthop. 2002 Feb;121(2):166-75; quiz 192. doi:10.1067/mod.2002.119435. PMID: 11840131.
12. Van Elslande D, Heo G, Flores-Mir C, Carey J, Major PW. Accuracy of mesiodistal root angulation projected by cone-beam computed tomographic panoramic-like images. Am J Orthod Dentofacial Orthop. 2010 Apr;137(4 Suppl):S94-9. doi: 10.1016/j.ajodo.2009.02.028. PMID: 20381767.
13. Garcia-Figueroa MA, Raboud DW, Lam EW, Heo G, Major PW. Effect of buccolingual root angulation on the mesiodistal angulation shown on panoramic radiographs. Am J Orthod Dentofacial Orthop. 2008 Jul;134(1):93-9. doi: 10.1016/j.ajodo.2006.07.034. PMID: 8617108.
14. Ali Alqerban, Reinhilde Jacobs, Steffen Fieuws, Guy Willems, Radiographic predictors for maxillary canine impaction, American Journal of Orthodontics and Dentofacial

Orthopedics, Volume 147, Issue 3 2015, Pages 345-354, ISSN 0889-5406, https://doi.org/10.1016/j.ajodo.2014.11.018.

15. Shapira Y., Kuftinec M.M. Early diagnosis and interception of potential maxillary canine impaction. *J Am Dent Assoc.* 1998;129:1450–1454.
16. Ericson S, Kurol J. Radiographic examination of ectopically erupting maxillary canines. *Am J Orthod Dentofacial Orthop.* 1988;91:483–92
17. Cernochova P, Izakovicova-Holla L. Dentoskeletal characteristics in patients with palatally and buccally displaced maxillary permanent canines. Eur J Orthod 2012;34:754-61.
18. Ludicke G, Harzer W, Tausche E. Incisor inclination—risk factor for palatally-impacted canines. J Orofac Orthop 2008;69:357-64.
19. . Bishara SE. Impacted maxillary canines: a review. Am J Orthod Dentofacial Orthop 1992;101:159-71.
20. . Peck S, Peck L, Kataja M. The palatally displaced canine as a dental anomaly of genetic origin. Angle Orthod 1994;64:249-56.
21. . Lai CS, Bornstein MM, Mock L, Heuberger BM, Dietrich T, Katsaros C. Impacted maxillary canines and root resorptions of neighbouring teeth: a radiographic analysis using cone-beam computed tomography. Eur J Orthod 2013;35:529-38.
22. Leonardi M, Armi P, Franchi L, Baccetti T. Two interceptive approaches to palatally displaced canines: a prospective longitudinal study. Angle Orthod. 2004 Oct;74(5):581-6. doi: 10.1043/0003-3219(2004)074<0581:TIATPD>2.0.CO;2. PMID: 15529490.
23. Ali Murat Aktan, Sami Kara, Faruk Akgünlü, Sıddık Malkoç, The incidence of canine transmigration and tooth impaction in a Turkish subpopulation, *European Journal of*

Orthodontics, Volume 32, Issue 5, October 2010, Pages 575–581, https://doi.org/10.1093/ejo/cjp151

24. Ericson S, Kurol J. Radiographic examination of ectopically erupting maxillary canines. *Am J Orthod Dentofacial Orthop.* 1988;91:483–92.
25. José Rubén Herrera-Atoche, María del Rosario Agüayo-de-Pau, Mauricio Escoffié-Ramírez, Fernando Javier Aguilar-Ayala, Bertha Arelly Carrillo-Ávila, Marina Eduviges Rejón-Peraza, "Impacted Maxillary Canine Prevalence and Its Association with Other Dental Anomalies in a Mexican Population", *International Journal of Dentistry*, vol. 2017, Article ID 7326061, 4 pages, 2017. https://doi.org/10.1155/2017/7326061
26. Brin I, Becker A, Shalhav M. Position of the maxillary permanent canine in relation to anomalous or missing lateral incisors: a population study. Eur J Orthod 1986;8:12-6.
27. Leonardi R, Muraglie S, Crimi S, Pirroni M, Musumeci G, Perrotta R. Morphology of palatally displaced canines and adjacent teeth, a 3-D evaluation from cone-beam computed tomographic images. BMC Oral Health 2018;18:156.
28. Cao D, Shao B, Izadikhah I, Xie L, Wu B, Li H, et al. Root dilacerations in maxillary impacted canines and adjacent teeth: a retrospective analysis of the difference between buccal and palatal impaction. Am J Orthod Dentofacial Orthop 2021;159: 167-74.
29. Kajan ZD, Sigaroudi AK, Nasab NK, Shafiee Z, Nemati S. Evaluation of diagnostically difficult impacted maxillary canines in orthodontic patients and its effect on the root of adjacent teeth using cone beam computed tomography. J Oral Maxillofac Radiol 2014;2:2.

30. Langberg BJ, Peck S. Adequacy of maxillary dental arch width in patients with palatally displaced canines. *Am J Orthod Dentofacial Orthop.* 2000;118:220–23

31. McConnell TL, Hoffman DL, Forbes DP, Jensen EK, Wientraub NH. Maxillary canine impaction in patients with transverse maxillary deficiency. *J Dent Child.* 1996;63:190–5.

32. Ericson S, Kurol J. Radiographic examination of ectopically erupting maxillary canines. *Am J Orthod Dentofacial Orthop.* 1988;91:483–92.

33. Sambataro S, Baccetti T, Franchi L, Antonini F. Early predictive variables for upper canine impaction as derived from posteroanterior cephalograms. *Angle Orthod.* 2005;75:28–34.

34. Fernandez E, Bravo LA, Canteras M. Eruption of the permanent upper canine: a radiologic study. *Am J Orthod Dentofacial Orthop.* 1998;113:414–20.

35. Papagiannis, A. and Halazonetis, D.J (2016) Shape variation and covariation of upper and lower dental arches of an orthodontic population. *European Journal of Orthodontics*,38 202-211

36. Klingenberg, C.P. (2010) Evolution and development of shape: integrating quantitative approaches. *Nature Reviews Genetics*, 11, 623–635

37. Liuti T, Dixon PM. The use of the geometric morphometric method to illustrate shape difference in the skulls of different-aged horses. Vet Res Commun. 2020 Nov;44(3-4):137-145. doi: 10.1007/s11259-020-09779-8. Epub 2020 Jul 23. PMID: 32700122; PMCID: PMC7568715.

38. Brin I, Becker A, Shalhav M. Position of the maxillary permanent canine in relation to anomalous or missing lateral incisors: a population study. Eur J Orthod 1986;8:12-6.

Publishing Agreement

It is the policy of the University to encourage open access and broad distribution of all theses, dissertations, and manuscripts. The Graduate Division will facilitate the distribution of UCSF theses, dissertations, and manuscripts to the UCSF Library for open access and distribution. UCSF will make such theses, dissertations, and manuscripts accessible to the public and will take reasonable steps to preserve these works in perpetuity.

I hereby grant the non-exclusive, perpetual right to The Regents of the University of California to reproduce, publicly display, distribute, preserve, and publish copies of my thesis, dissertation, or manuscript in any form or media, now existing or later derived, including access online for teaching, research, and public service purposes.

DocuSigned by:
Stephen Kasper
2D2D2928803B4BA...
Author Signature

5/26/2023
Date